Journal of ELECTRONIC MATERIALS, Vol. 49, No. 12, 2020
https://doi.org/10.1007/s11664-020-08526-8

Growth and Characterization of Single Crystals of L-Histidine Hydrochloride Monohydrate for Nonlinear Optical Applications

SUDHA YADAV,[1,2] MANJU KUMARI,[1,2] DEBABRATA NAYAK,[1,2] SABYASACHI BANERJEE,[4] NAGHMA KHAN,[1,2] SUBHASH NIMANPURE,[1,2] GIRIJA MOONA,[2] RINA SHARMA,[1,2] BHUPENDRA K. SHARMA,[3] DIBAKAR ROY CHOWDHURY,[4] N. VIJAYAN,[1,2] and MUKESH JEWARIYA[1,2,5]

1.—Academy of Scientific and Innovative Research (AcSIR), CSIR-HRDC Campus, Ghaziabad, Uttar Pradesh 201002, India. 2.—CSIR-National Physical Laboratory, Dr. K.S. Krishnan Road, New Delhi 110012, India. 3.—Department of Science and Technology, Technology Bhavan, New Mehrauli Road, New Delhi 110016, India. 4.—Mahindra École Centrale, Hyderabad, Telangana 500043, India. 5.—e-mail: jewariya.mukesh@nplindia.org

In the present study, we have focused on the growth of semi-organic single crystals, as they play a vital role in the generation of a terahertz pulse and its potential applications. The single crystals of L-histidine hydrochloride monohydrate (LMHCL) were grown by slow evaporation solution growth by using deionized water as a solvent in a controlled atmosphere. Good quality crystals of the required size were obtained within 2 weeks. To estimate the lattice dimensions and get the structural information, powder x-ray diffraction (PXRD) study was performed in which we have found that the crystal belongs to the orthorhombic crystal system with space group $P2_12_12_1$. The functional groups and the corresponding vibrational mode were confirmed using Fourier transform infrared (FTIR) and Raman spectroscopy, respectively. To study the optical properties UV–Vis transmission spectrum and photoluminescence (PL) were recorded. It was observed that the single crystal has a high value of transmission over a long range of wavelength which signifies that the crystal is a good candidate for nonlinear optical (NLO) applications. The UV cut-off wavelength is found to be 236 nm. The grown single crystals were studied by time-domain terahertz spectroscopy (THz-TDS) for photonic applications and the refractive indices were calculated and it is found that the refractive index is nearly equal to 3.4.

Key words: Terahertz, powder x-ray diffraction, photoluminescence, single crystal, optical

INTRODUCTION

Recently, nonlinear optical (NLO) crystals are of increasing importance and find a greater consideration because of their potential applications in terahertz (THz) generation, THz imaging & spectroscopy, laser amplifiers, ultrafast switches, optical devices, etc. in everyday life.[1] Synthesizing, engineering, and designing these new nonlinear optical (NLO) materials are a major research focus for scientists and researchers.[2] Among these materials, single crystals are one of the most prominent and outstanding NLO materials due to their prime optical quality. In this regard, amino acid-based single crystals are fascinating materials for NLO applications as the amino acids contain one proton donor carboxyl group and a protonated amine group. This ionic nature favors the special physical and chemical properties in these acids such as crystal hardness and high nonlinear susceptibility

(Received June 27, 2020; accepted September 25, 2020; published online October 18, 2020)

(χ^2) which make them potential candidates for NLO applications.[3] Nowadays, THz spectroscopy is also becoming an active and ambitious research field because almost all materials have terahertz response below 1 THz. NLO has numerous applications in terms of single crystals such as detection of polymorphism in food and drugs, THz imaging, spectroscopy, and non-destructive security inspection, and detection of inter- and intramolecular bonds. These applications are only possible due to various NLO-based sources and detectors in the terahertz frequency region.[4] Recent reports in research show that many amino acid-based NLO crystals such as L-histidine are the focus of current studies. This amino acid is very crucial, having an imidazole ring which is known to be the active center of several enzymes, uses protein and manages the communication of metal elements on the basis of biology[5] which gives different various derivatives for NLO applications such as L-histidine tetrafluoroborate, a new novel NLO material.[6,7] The structural information of L-histidine dihydrochloride was analyzed and reported previously,[8] whereas structural properties and THz time-domain spectroscopy of L-histidine hydrochloride monohydrate have been studied recently using density functional theory (DFT).[9] In our present study, we have grown L-histidine hydrochloride monohydrate single crystals and observed their structural properties. We have reported the photoluminescence studies for the first time for this material. THz time-domain spectroscopy of L-histidine hydrochloride monohydrate was studied and the refractive index of the crystal was also calculated. To the best of our knowledge, these results have never been reported. The derivative of L-histidine, L-histidine hydrochloride monohydrate (LMHCL) which is a semi-organic material having chemical formula $C_6H_{12}ClN_3O_3$ with a non-centrosymmetric space group $P2_12_12_1$, is used for single crystal growth. The slow evaporation solution growth technique (SEST) was used to harvest the mentioned material.

EXPERIMENTAL

Crystal Growth

Single crystals of LMHCL were grown by slow evaporation solution growth technique (SEST). The commercially available LMHCL (99% pure) was taken as a solute and de-ionized water as a solvent as the host material had good solubility with it. They were mixed together and stirred continuously using a magnetic stirrer at a constant speed for about 2 h until a saturated solution was obtained. As the purity in the compound is the most important trait to enhance the quality of crystals, the purity of the compound was improved by repetitive crystallizations to get the superior optical quality crystals. The prepared solution was filtered using Whatman filter paper and covered with a thin, perforated sheet for evaporation purposes. The filtered solution was put in a thermally controlled atmosphere using a constant temperature bath.[10,11] After successive recrystallization, a crystal of good quality was harvested with a span of 14 days. The dimensions of the crystal were measured using a length measuring machine (LMM), Model OPAL 1000 with a range of 0–1000 mm. The dimensions of the grown crystal were found to be 1.8 cm × 1.5 cm × 0.3 cm. The optically transparent, nonhygroscopic, and good quality grown crystal with dimensions (1.8 cm × 1.5 cm × 0.3 cm) is shown in Fig. 1.[12]

RESULTS AND DISCUSSION

Powder X-ray Diffraction Analysis

Powder x-ray diffraction (PXRD) analysis of the grown crystal was carried out to find the lattice parameters, structure, and phase identification.[13] The powdered sample crushed by agate mortar was put into a Rigaku (Ultima–IV) x-ray diffractometer using with Cu K-alpha radiation as a source with a wavelength λ = 1.541836 Å.[14] The measurements were made in the 2θ range of 10°–50°. The recorded PXRD diffraction data is enfolded in the mentioned Fig. 2. The all intense peak is indexed and the diffraction pattern of LMHCL is efficiently matched with the reported one.[15,16] Refined unit cell dimensions was found as a = 6.8434 Å, b = 8.9401 Å, c = 15.2763 Å.[6] The mentioned crystal belongs to the orthorhombic crystal system with non-centrosymmetric space group $P2_12_12_1$ which is a significant need for the second harmonic efficiency applications.[17]

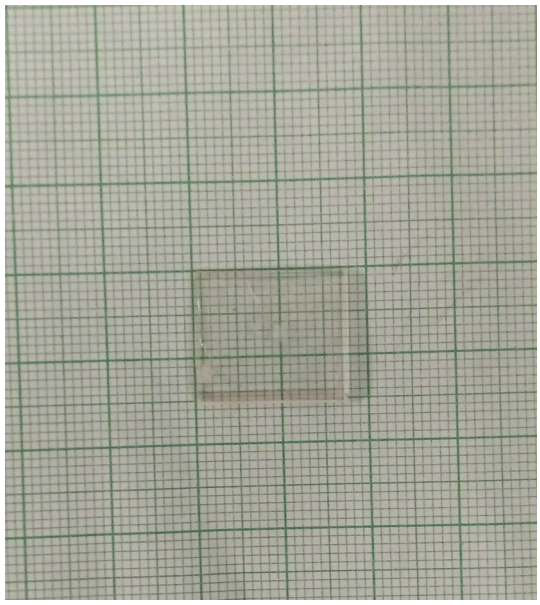

Fig. 1. LMHCL single crystal.

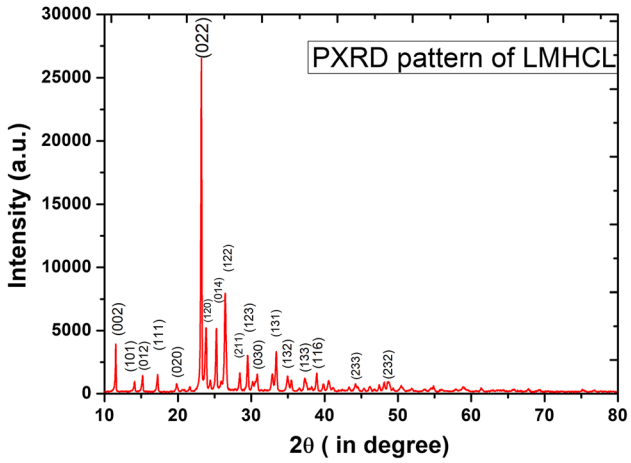

Fig. 2. PXRD pattern of LMHCL.

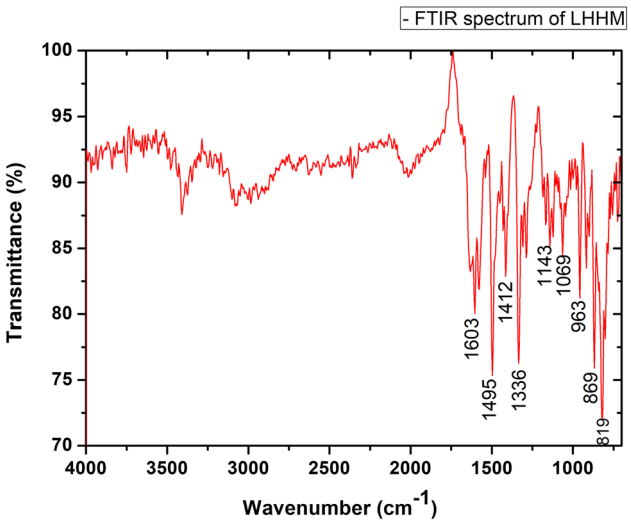

Fig. 3. FTIR spectrum of LMHCL.

FTIR and FT-Raman studies

The presence of several fundamental groups and vibrational modes in the host compound was assessed through an infrared spectrum and Raman spectroscopy. A Nicolet 5700 spectrometer was used to find the spectral range for the FTIR analyses from 400 cm^{-1} to 4000 cm^{-1} . The recorded spectra are given in Figs. 3 and 4. One can see from Fig. 3 that the N–H symmetric stretching, C-H stretching and CH_2 asymmetric stretching lies at 3151 cm^{-1}, 3012 cm^{-1}, and 2949 cm^{-1} , respectively. The symmetric bend of NH_3^+ lies at 1483 cm^{-1} in the FTIR spectrum and at 1495 cm^{-1} in the FT-Raman spectrum.[6,7,15,18] The detailed comparative assignments for the compound are tabulated below in Table I.[19,20]

UV–Vis Analysis

To find the optical properties, structural information, and transmission of the grown ingot, UV–Vis

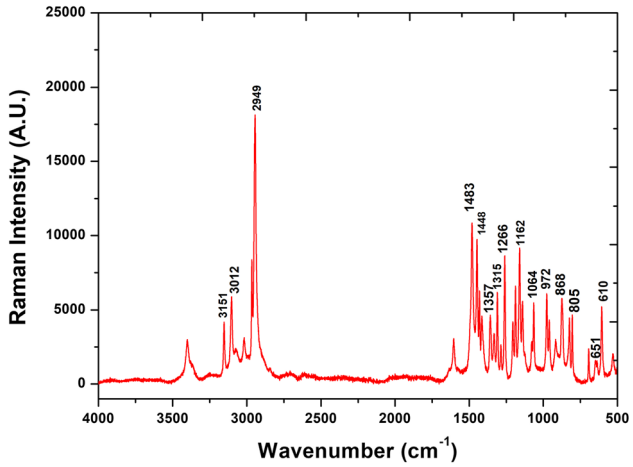

Fig. 4. Raman spectrum of LMHCL.

spectra were recorded, as highly transparent crystals play a vital role in optoelectronic, photonics, and NLO applications. The experimental recorded optical transmission spectrum of the crystal is shown in Fig. 5. It can be found that the transparency of the crystal is about 80% and the UV cut-off wavelength is 236 nm. The low value of cut-off wavelength with a high range of transmission signifies the importance of the LMHCL crystal for optoelectronic and NLO applications.[21]

To examine the material strength for optoelectronic application, it is important to find the optical constants. The value of absorption coefficient (α) can be evaluated by using transmittance (T) and thickness (t) of grown crystals, as given in below Eq. 1:[22]

$$\alpha = \frac{2.3026}{t}\log\left(\frac{1}{T}\right) \quad (1)$$

Now the optical band gap E_g can be obtained by the following expression

$$\alpha h\upsilon = B\left(h\upsilon - E_g\right)^n \quad (2)$$

Here, n determines the nature of transitions taking place (n = 2 for allowed indirect transitions and n = 1/2 for allowed direct transitions), B is constant and $h\upsilon$ is the photon energy.[23] Now using Tauc's plot (graph of $(\alpha h\upsilon)^2$ versus $h\upsilon$) band gap of the crystal was calculated and found to be 5.13 eV. The plot for the band gap is shown in Fig. 6.

Photoluminescence Properties

Photoluminescence (PL) spectroscopy is an effective characterization tool to detect imperfections, the density of colour centres, defects, to determine band gap, etc. It is commonly done using high-energy photons in excited valence electrons of the material from the ground state to the excited states. In this way, we can find the defects present in the material from the recorded emission spectrum. For the abovementioned crystal, PL measurements were examined using Edinburgh instruments

Table I. Wavenumber and assignments for FTIR and FT-Raman spectra

Wavenumber (cm^{-1}) FTIR	Wavenumber (cm^{-1}) FT-Raman	Assignment
3151	–	N-H symmetric stretching
3012	–	C-H stretching
2949	–	CH_2 asymmetric stretching
–	1603	Asymmetric bend of NH_3^+ and C=N stretching
1483	1495	Symmetric bend of NH_3^+
1448	–	Ring deformation
–	1412	Symmetric mode of -COO^- and C-N stretching
–	1336	CH_2 bending
1357	–	CH_2 deformation
1315	–	C-N stretching
1266	–	C-C and C=O stretching
1162	1143	C-H in plane bending
1064	1069	C-O stretching of COO^- group
972	963	O-H stretching of carboxylic acid
868	869	C-N deformation
805	819	Ring deformation
651	–	C=O deformation
610	–	Ring deformation or C-N deformation

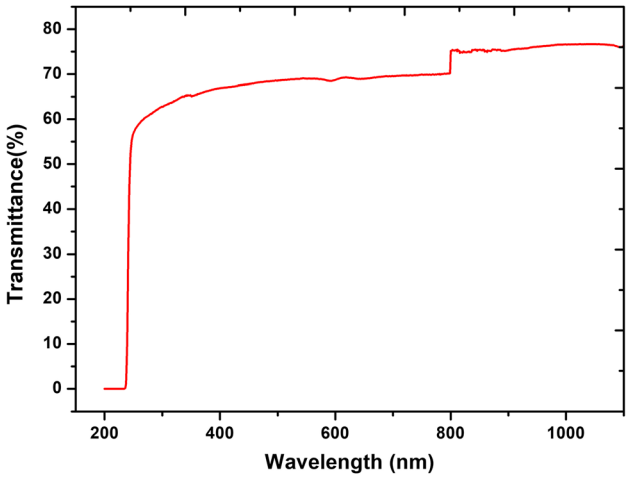

Fig. 5. UV-Vis spectral analysis.

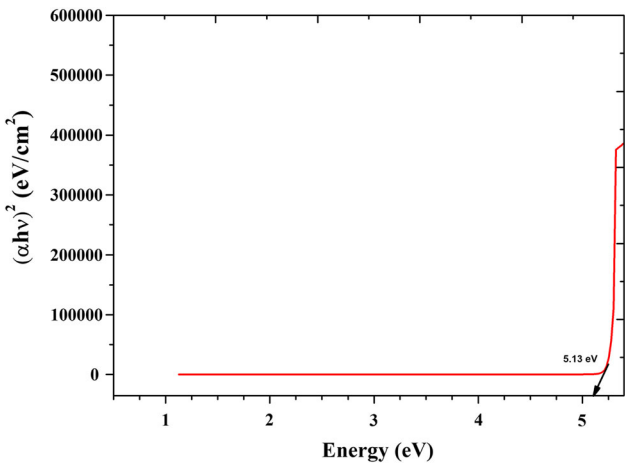

Fig. 6. Graph of $(\alpha h\upsilon)^2$ versus photon energy ($h\upsilon$).

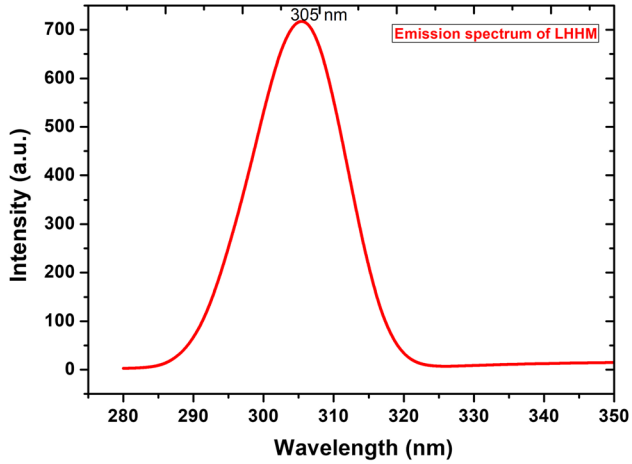

Fig. 7. PL spectrum.

(FLS-980, D2D2).[24]. In this setup, firstly the LMHCL crystal was excited using a xenon flash lamp at 270 nm in ambient conditions, and the spectrum was recorded in the range of 270–600 nm, as shown in Fig. 7, in which one can see that there are no extra peaks and a single intensified emission peak is observed at 305 nm for the excitation wavelength of 270 nm. The results indicate that the crystal is defect-free and have single-crystalline nature. It also reveals the utility of LMHCL in practical applications.

Terahertz Spectroscopy

The high-quality LMHCL single crystal was studied further through terahertz time-domain spectroscopy in transmission mode. The schematic representation of the interaction of incident THz pulse with LMHCL crystal is mentioned in Fig. 8.

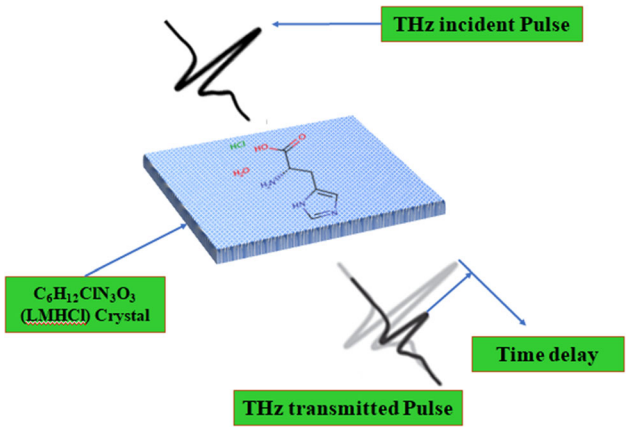

Fig. 8. Interaction of THz pulses with LMHCl crystal.

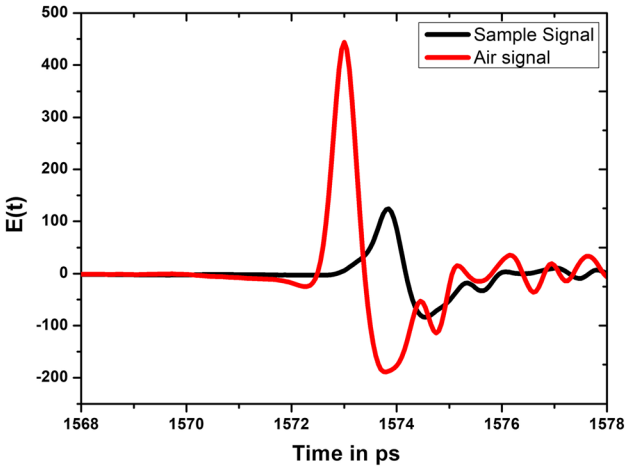

Fig. 9. Reference signal and sample signal versus time graph.

When the THz pulses are incident on LMHCL crystal, some THz radiation is absorbed, some reflected and the rest transmitted through the LMHCl crystal. In the THz-TDS experiment, a signal proportional to the electric field of the THz pulse $E(t)$ is used. To find the frequency, the Fourier transform is obtained from the time-domain signals (Fig. 9, 10).

$$E(\omega) = \frac{1}{2\pi}\int_{-\infty}^{+\infty} \mathrm{e}^{-i\omega t}E(t)\mathrm{d}t \qquad (3)$$

Two traces are recorded in the THz transmission spectroscopy experiment in which one where the pulse propagates through the sample and the other as a reference pulse propagated through the bare substrate, E_{sam} and E_{ref}, respectively. From the captured data it is possible to extract information about the response time, frequency spectra, absorption coefficient and optical density for particular devices and samples (Fig. 11).

The reference wave propagating through vacuum ($n = 1$, $k = 0$) of the same length as shown in Fig. 12, is given by Eq 4.

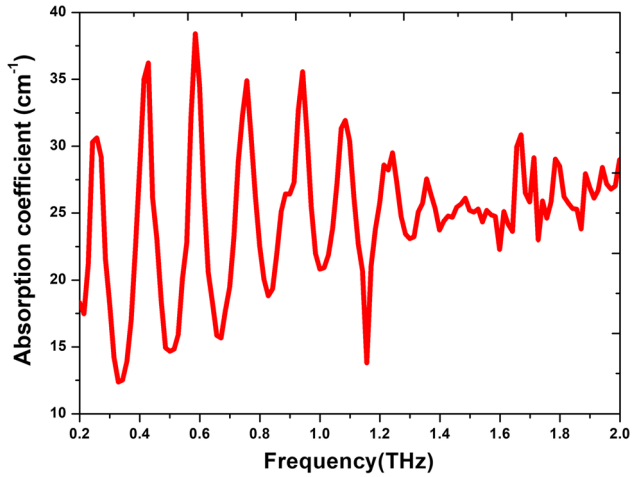

Fig. 10. FFT amplitude spectrum.

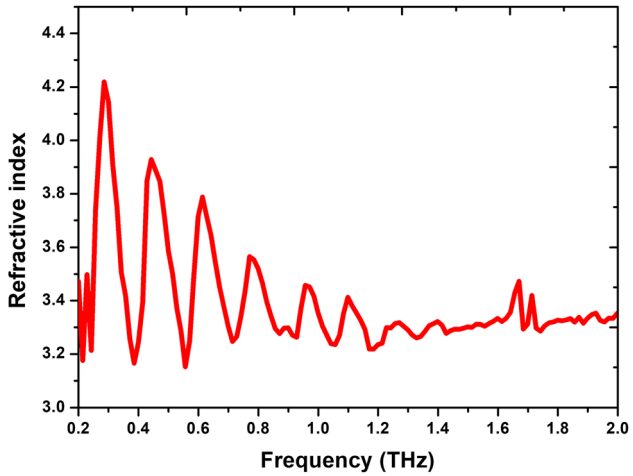

Fig. 11. Refractive index versus Frequency graph.

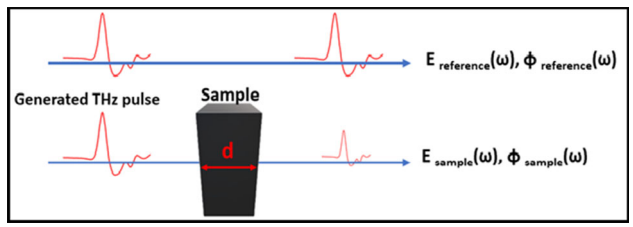

Fig. 12. The basic scheme of a THz-time domain spectroscopy transmission experiment.

$$E_{\mathrm{ref}}(\omega) = E_o(\omega)\exp\left\{i\frac{\omega}{c}d\right\} \qquad (4)$$

Now, the absorption and dispersion across the medium causes a change in the THz field. Thus, after propagation, the frequency-dependent field through the MWCNT-FP sample is given by Eq 5.

$$E_{\text{sam}}(\omega) = E_o(\omega)T\exp\left\{i\left(\frac{n(\omega)\omega}{c}\right)d\right\} \cdot \exp\left\{\left(\frac{k(\omega)\omega}{c}\right)d\right\} \quad (5)$$

where $n(\omega)$ and $k(\omega)$ are the refractive indices of MWCNT-FP sample and T is the transmission amplitude coefficient. It is given by

$$T = \frac{n(\omega)}{\{n(\omega)+1\}^2} \quad (6)$$

The frequency-dependent complex ratio is called by transmission and can be determined by the Eqs 4 and 5.

$$\text{Trans} = \frac{E_{\text{sam}}(\omega)}{E_{\text{ref}}(\omega)} = \frac{n(\omega)}{\{n(\omega)+1\}x^2}\exp\left\{-\left(\frac{k(\omega)}{c}\right)d\right\} \cdot \exp\left\{i\left(\frac{n(\omega)-1}{c}\right)\omega d\right\} \quad (7)$$

So, the transmission intensity is defined as

$$I_{\text{trans}} = I_{\text{in}}e^{-\alpha\cdot d}$$

where

$$I_{\text{trans}} = |E_{\text{sam}}|^2 \text{ and } I_{\text{in}} = |E_{\text{ref}}|^2$$

Thus, the ratio of transmitted and incident intensity can easily obtain according to Eq. 5 and defined as

$$\alpha = -\frac{2}{d}\text{In}(\text{Trans}) \quad (8)$$

where α is the absorption coefficient and if the base of exponential function is 10, then it is defined as optical density.[25].

From the spectra, it is concluded that the small dips were due to the multiple reflections of THz waveforms from both edges of the crystals found using a Fabry-Perot interferometer. Above 1.5 THz, the peaks were due to the noise in the system. The sharp spectral peaks nearly equal to 1 THz are due to the absorption of clusters of water molecules in the setup. From 0.2 THz to 2 THz, the dips shows the intermolecular interactions between the molecule.[26–28]

By the formula mentioned below in Eq. 9, we calculated the refractive index (n) of the above compound and its a graph of refractive index versus frequency is shown in given Fig. 11.

$$n = 1 + \frac{\Delta\Phi c}{\omega t} \quad (9)$$

where ϕ is a phase difference, c is the velocity of light ω is frequency and t is the thickness of the sample used. The refractive index of the above compound is nearly equal to 3.4.

CONCLUSIONS

High optical quality single crystals of LMHCl have been grown by adopting slow evaporation solution growth. Crystal structure and lattice cell parameters are confirmed by using PXRD and it is revealed that the crystal is non-centrosymmetric with space group $P2_12_12_1$. Functional groups and vibrational modes existing in the ingot have been examined by FTIR and Raman spectroscopy. The transparency of the crystal was checked by using UV–Vis spectroscopy and it was about 80% with a cut-off wavelength of 236 nm. There was no absorption of light in the visible region of the EM spectrum. From Tauc's plot, the energy band gap is found to be 5.13 eV. From PL studies it is understood that the crystal is free from defects. The ingot crystal is studied using terahertz spectroscopy and periodic behaviour is observed due to repeated functional groups. This crystal has the ability to generate a THz pulse, but first we must analyse its properties in THz frequency region. The refractive index of the material was estimated to be 3.4. The intermolecular interactions of the material were studied in terahertz region. It revealed that LMHCL is very efficient THz material for upcoming practical applications.

ACKNOWLEDGMENTS

The authors are thankful to Director, CSIR-NPL for his continuous encouragement in carrying out the present study. One of the authors Ms. SY is thankful to CSIR for giving financial support through CSIR-Junior Research fellowship (JRF) and also to AcSIR-NPL for Ph.D. registration. Author MJ acknowledges SERB, New Delhi, India, for the financial support provided by with reference No. SB/EMEQ-022/2014-2019.

CONFLICT OF INTEREST

The authors declare no conflict of interest.

REFERENCES

1. M. Amalanathan, I. Hubert Joe, and V.K. Rastogi, *J. Mol. Struct.* 985, 48–56 (2011).
2. N.V. Sonia, M. Vij, K. Thukral, N. Khan, D. Haranath, and M.S. Rajnikant, *Chin. J. Chem. Eng.* 27, 701–708 (2018).
3. S. Moitra and T. Kar, *J. Cryst. Growth* 310, 4539–4543 (2008).
4. M. Jazbinsek, U. Puc, A. Abina, and A. Zidansek, *Appl. Sci.* 9, 882 (2019).
5. G.N. Chen, X.P. Wu, J.P. Duan, and H.Q. Chen, *Talanta* 49, 319–330 (1999).
6. P. Anandan, M. Arivanandhan, Y. Hayakawa, D. Rajan Babu, R. Jayavel, G. Ravi, and G. Bhagawannarayana, *Spectrochim. Acta A Mol. Biomol. Spectrosc.* 121, 508–513 (2014).
7. H.O. Marcy, L.A. DeLoach and J.H. Liao, *Opt. Lett.* 20, 252–254 (1995).

8. T.J. Kistenmacher and T. Sorrell, *J. Cryst. Mol. Struct.* 4, 419–432 (1974).
9. S. Zong, G. Ren, S. Li, B. Zhang, J. Zhang, W. Qi, J. Han, and H. Zhao, *J. Mol. Struct.* 1157, 489–491 (2018).
10. P. Anandan and R. Jayavel, *J. Cryst. Growth* 322, 69–73 (2011).
11. K. Srinivasan, K. Meera, and P. Ramasamy, *J. Cryst. Growth* 205, 457–459 (1999).
12. N. Vijayan, J. Philip, D. Haranath, B. Rathi, G. Bhagavannarayana, S.K. Halder, N. Roy, M.S. Jayalakshmy, and S. Verma, *Spectrochim. Acta A Mol. Biomol. Spectrosc.* 122, 309–314 (2014).
13. S.K. Kurtz and T.T. Perry, *J. Appl. Phys.* 39, 3798 (1968).
14. M. Vij, H.K. Sonia, M.S. Verma, B. Jayalakshmy, S.Verma Singh, and K.K. Maurya, *Phys. B* 550, 250–259 (2018).
15. P. Anandan, R. Jayavel, T. Saravanan, G. Parthipan, C. Vedhi, and R. Mohan Kumar, *Opt. Mater.* 34, 1225–1230 (2012).
16. G.R. Ester and P.J. Halfpenny, *J. Cryst. Growth* 187, 111–118 (1998).
17. R. Robert, C. Justin Raj, S. Krishnan, R. Uthrakumar, S. Dinakaran, and S. Jerome Das, *Phys. B* 405, 3248–3252 (2010).
18. J. Madhavan, S. Aruna, P.C. Thomas, M. Vimalan, S.A. Rajasekar, and P. Sagayaraj, *Cryst. Res. Technol.* 42, 59–64 (2007).
19. R. Ittyachan and P. Sagayaraj, *J. Cryst. Growth* 249, 557 (2003).
20. E.D. D'silva, G.K. Podagatlapalli, S.V. Rao, and S.M. Dharmaprakash, *Opt. Laser Technol.* 44, 1689–1697 (2012).
21. S.A. MartinBrittoDhas, M. Suresh, G. Bhagavannarayana, and S. Natarajan, *J. Cryst. Growth* 309, 48–52 (2007).
22. IUPAC. Compendium of Chemical Terminology, 2nd ed. (the "Gold Book"). Compiled by A. D. McNaught and A. Wilkinson. Blackwell Scientific Publications (1997).
23. K. Moovendaran and S. Natarajan, *J. Appl. Crystallogr.* 46, 993–998 (2013).
24. M. Kumari, N. Vijayan, D. Nayak, M. Kumar, G. Gupta, and R.P. Pant, *Mater. Res. Express* 7, 015705 (2020).
25. Mukesh Jewariya, D.Sc. Thesis, "Resonant Excitation of Large Amplitude Anharmonic Vibrations of Amino acids Micro Crystals by an Intense Monocycle Terahertz Pulse" Kyoto University, Kyoto, Japan, 2010.
26. V. Krishnakumar and R. Nagalakshmi, *Cryst. Growth Des.* 11, 3882–3884 (2008).
27. S. Karthick, D. Ganesh, K. Thirupugalmani, A.K. Chaudhary, and S. Brahadeeswaran, *Mater. Lett.* 246, 95–98 (2019).
28. A. Ashour, N. El-Kadry, and S.A. Mahmoud, *Thin Solid Films* 269, 117–120 (1995).